Magneto-optical coupling in ferromagnetic thin films investigated by vector-magneto-optical generalized ellipsometry

K. Mok,[1,*] G. J. Kovács,[1] J. McCord,[1,2] L. Li,[1] M. Helm,[1] and H. Schmidt[1]
[1]*Institute of Ion Beam Physics and Materials Research, Helmholtz-Zentrum Dresden-Rossendorf (HZDR), P.O. Box 510119, D-01314 Dresden, Germany*
[2]*Institute for Materials Science, University of Kiel, Kaiserstrasse 2, 24143 Kiel, Germany*
(Received 3 June 2011; revised manuscript received 16 August 2011; published 15 September 2011)

We performed generalized Mueller matrix ellipsometry measurements in a magnetic field of arbitrary orientation and magnitude up to 400 mT at room temperature and probed the magneto-optical response of capped, ferromagnetic Fe, $Ni_{20}Fe_{80}$, Co, $Ni_{80}Fe_{20}$, and Ni thin films on ZnO substrates in the spectral range from 300 to 1100 nm. We determined the off-diagonal elements in the magneto-optical dielectric tensor under saturated magnetization conditions in the sample surface plane via a model analysis. The off-diagonal elements depend on the net spin polarization and the electronic band structure of the ferromagnetic thin films. For the pure ferromagnetic metals Fe, Co, and Ni, the converted off-diagonal elements agree well with the reported experimental optical conductivity data. As a result we use the extracted wavelength-dependent magneto-optical coupling constant to predict the wavelength-dependent magneto-optical response of different Ni/Fe multilayer structures.

DOI: 10.1103/PhysRevB.84.094413 PACS number(s): 78.20.Ls, 75.70.−i, 78.30.Er

I. INTRODUCTION

During the last decades, the magneto-optical (MO) properties of Co, Fe, Ni, and their alloys have been extensively studied due to their technological potential in data storage devices and sensor applications. Also metallic multilayer stacks in giant and tunnel magnetoresistance structures have been characterized by means of nondestructive MO measurements. The MO properties of ferromagnetic materials are uniquely given by their respective complex MO dielectric tensor ε^{MO}. Under saturated magnetization conditions, the wavelength-dependent and magnetic-field-independent MO coupling constant $\mathbf{Q}$ can be determined.[1] This MO coupling constant depends on the net spin polarization and electronic band structure of magnetizable materials. Magneto-optical Kerr effect (MOKE) is the most widely used method for MO characterization so far. Oppeneer *et al.*,[2] Gasche *et al.*,[3] and Delin *et al.*[4] have calculated the MOKE signal of Co, Fe, and Ni under saturated magnetization conditions. Mertins *et al.*[5] reported the experimental longitudinal Kerr spectra measured at the $2p$ absorption edges of Co, Fe, and Ni in the spectral range from 600 to 900 nm. However, a clear interpretation of the MO coupling constant $\mathbf{Q}$ in terms of the net spin polarization and electronic band structure has not been done.

Recently, magneto-optical generalized ellipsometry (MOGE) has been developed to study layered samples with optical anisotropy induced by an external magnetic field.[6–9] Not only measuring the MOKE of a sample, MOGE also allows one to perform generalized Mueller matrix ellipsometry, which provides a MO analysis of arbitrarily anisotropic and depolarizing magnetic multilayer samples.[9] In order to determine the off-diagonal elements of the complex MO dielectric tensor ε^{MO}, MOKE measures the Kerr rotation and ellipticity in a magnetic field, while MOGE allows one to measure more than two magnetic-field-dependent parameters, namely up to 16 Mueller matrix elements. This advantage of MOGE allows one to better fit the unique wavelength-dependent ε^{MO} of every layer in the multilayer sample under saturated magnetization conditions with more experimental parameters. The present work is organized as follows: In Sec. II A, the vector-magneto-optical generalized ellipsometry (VMOGE)[1] technique is presented. The optical and magnetic properties, as well as the structure of the investigated multilayer sample with ferromagnetic thin films are discussed in Sec. II B. In Sec. III we model the Mueller matrix data obtained from VMOGE measurements under saturated magnetization conditions in the $\{xy\}$-sample surface plane and relate the wavelength-dependent, complex MO coupling constants Q_x and Q_y with experimental optical conductivity data of ferromagnetic thin films. We conclude our work in Sec. IV.

II. EXPERIMENT

A. Vector-magneto-optical generalized ellipsometry

VMOGE is a MO characterization technique that uses a generalized spectroscopic ellipsometer combined with an octupole magnet. A custom designed octupole magnet sample stage from Anderberg & Modéer Accelerator AB, Sweden is mounted onto a rotating analyzer ellipsometer VASE (J. A. Woollam Co., Inc., USA). This setup allows one to perform generalized ellipsometry experiments at room temperature under field-free conditions, as well as on magnetized samples. The Mueller matrix of reflected and transmitted light can be measured as a function of wavelength from 300 nm to 1100 nm and of an arbitrarily oriented magnetic field with magnitudes up to 400 mT. During the measurement, changing the magnetic field direction does not require moving the sample and hence further sample alignment and calibration are not needed. The presented VMOGE setup allows one to determine 11 Mueller matrix elements M_{ij}, $i = 1,2,3$, $j = 1,2,3,4$, normalized to the Mueller matrix element M_{11}. The fourth row of the Mueller matrix (M_{41}, M_{42}, M_{43}, M_{44}) is not accessible due to the fact that the rotating analyzer ellipsometer used in our VMOGE setup contains only one compensator. However, this does

 ©2011 American Physical Society

not impair the accessibility of the normalized Mueller matrix elements, except for their absolute phase.[10,11]

In the VMOGE setup, a Cartesian coordinate system is defined with the z axis normal to the interfaces and pointing into the substrate from the sample surface. The x and z axis lie in the plane of incidence. Three VMOGE configurations: longitudinal (L), transverse (T), and polar (P) are defined according to the direction of applied magnetic field vector $\mathbf{H} = (H_x, H_y, H_z)$. In the L-VMOGE configuration, $\mathbf{H}$ is parallel to both the sample surface and the plane of incidence. In the T-VMOGE configuration, $\mathbf{H}$ is parallel to the sample surface and perpendicular to the plane of incidence. In the P-VMOGE configuration, $\mathbf{H}$ is perpendicular to the sample surface. For $\mathbf{H}$ within the Cartesian coordinate system of the VMOGE setup, the MO properties of the ferromagnetic thin films in the investigated Cr/ferromagnetic thin film/ZnO substrate layered systems are described by the following MO dielectric tensor $\varepsilon^{\mathrm{MO}}$:

$$\varepsilon^{\mathrm{MO}} = \begin{bmatrix} \varepsilon_x & -iQ_zM_z & -iQ_yM_y \\ iQ_zM_z & \varepsilon_y & -iQ_xM_x \\ iQ_yM_y & iQ_xM_x & \varepsilon_z \end{bmatrix}, \qquad (1)$$

where the diagonal terms $\varepsilon_{x,y,z}$ are the square of the complex refractive index, and the off-diagonal, nonsymmetric terms $\varepsilon_{ij}^{\mathrm{MO}}$ are assumed to depend on the magnetization $\mathbf{M} = (M_x, M_y, M_z)$ and the complex MO coupling constant $\mathbf{Q} = (Q_x, Q_y, Q_z)$. It is important to clarify that there exist different sign conventions to describe the MO dielectric tensor. According to the optics convention of optical constants,[11] the MO coupling constant is defined as $\mathbf{Q} = Re(\mathbf{Q}) - i\,Im(\mathbf{Q})$. The magnetization $\mathbf{M}$ of the investigated samples is parallel to the magnetic field $\mathbf{H}$ (i.e., $\mathbf{M} \parallel \mathbf{H}$). For example in L-VMOGE with $\mathbf{H} = (H_x, 0, 0)$, it holds that $\mathbf{M} = (M_x, 0, 0)$. The motivation for assuming the off-diagonal terms $\varepsilon_{ij}^{\mathrm{MO}} \propto Q_k M_k$ with $k = x, y, z$ is to determine magnetic-field-independent MO coupling constant $\mathbf{Q}$ and to distinguish between the anisotropy of $\mathbf{Q}$ and $\mathbf{M}$. The off-diagonal terms in the dielectric tensor of the nonmagnetic Cr capping layer and the ZnO substrate are set to be zero.

The nondepolarizing Mueller matrix is modeled by the 4×4 transfer matrix method via the Jones matrix formalism[11–15] using the dielectric tensor of every layer in the multilayer sample, particularly, $\varepsilon^{\mathrm{MO}}$ for the ferromagnetic thin films. $\varepsilon_{ij}^{\mathrm{MO}}$ can be converted into the corresponding off-diagonal element $\sigma_{ij}^{\mathrm{MO}}$ of the optical conductivity tensor[16]

$$\sigma_{ij}^{\mathrm{MO}} = -i\omega\varepsilon_{ij}^{\mathrm{MO}}/4\pi, \qquad (2)$$

and we compare the $\omega\sigma_{ij}^{\mathrm{MO}}$ spectra to the experimental spectra reported in Refs. 2,4,17–24. Note that the model analysis allows one to determine the off-diagonal terms $\varepsilon_{ij}^{\mathrm{MO}}$, which reflect the MO figure of merit of ferromagnetic materials. The MO coupling constants $\mathbf{Q}$ and the magnetization $\mathbf{M}$ (Eq. (1)) cannot be determined independently. Hence, additional experiments are required to measure the magnetization $\mathbf{M}$ of the sample (e.g., by vector magnetometry). In order to obtain magnetic-field-independent MO coupling constants, $\mathbf{M}$ has to be factored out from the modeled off-diagonal terms $\varepsilon_{ij}^{\mathrm{MO}}$. In order to enhance the MO figure of merit of MO sensors in a given spectral range, it is important to choose sensor materials with a large MO coupling constant in this spectral range.

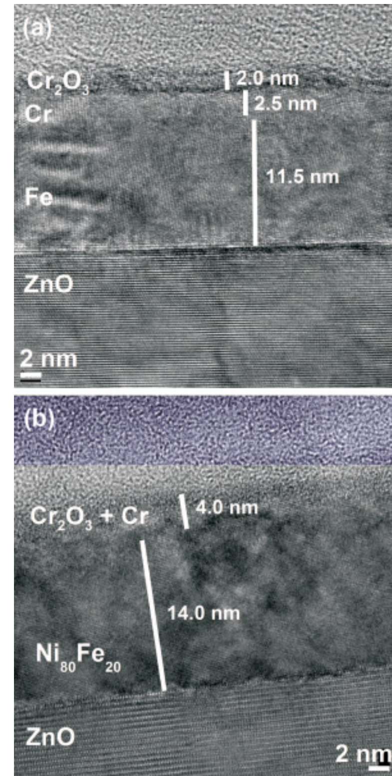

FIG. 1. (Color online) TEM images of the (a) Fe and (b) $Ni_{80}Fe_{20}$ thin film samples. The Fe and $Ni_{80}Fe_{20}$ thin films have bcc and fcc crystal structure, respectively. The Cr capping layer is partially oxidized, forming a 1–3 nm thick Cr_2O_3 layer.

B. Samples

The ferromagnetic Fe, $Ni_{20}Fe_{80}$, Co, $Ni_{80}Fe_{20}$, and Ni thin films have been deposited on annealed O-face ZnO substrates by electron beam evaporation. The nominal film thickness is 10 nm. A nominal 3-nm thick Cr capping layer has been deposited on top. The Cr layer partially oxidizes after deposition, and prevents oxidation of the underlying ferromagnetic films. For example, the oxidation of an uncapped Ni thin film results in the formation of antiferromagnetic NiO and may affect the MO response of the Ni sample as has been shown in Ref. 25. $Ni_{80}Fe_{20}$ and $Ni_{20}Fe_{80}$ thin film samples were investigated by Rutherford backscattering spectrometry (RBS) and it confirmed the expected Ni_xFe_{100-x} alloy compositions with $x =$ 80 and 20, respectively. Transmission electron microscopy (TEM) was used to study the crystalline structure and the layer thickness of Fe, $Ni_{80}Fe_{20}$, and Ni thin film samples. As an example, Fig. 1 shows the TEM images of the Fe and $Ni_{80}Fe_{20}$ thin film samples. The Fe and $Ni_{80}Fe_{20}$ thin films have bcc and fcc crystal structure, respectively. The structure of Ni thin film is basically similar to $Ni_{80}Fe_{20}$, which is fcc (image is not shown here). The thicknesses of Fe, $Ni_{80}Fe_{20}$, and Ni films determined by TEM are listed in Table I. In Fig. 1, we see that the Cr thickness ranges from 2 to 4 nm, an oxide layer Cr_2O_3 with thickness between 1 and 3 nm forms on top of Cr. The Cr capping layer is not completely oxidized, however it does not affect the MO properties of the underlying ferromagnetic thin films as long as the ferromagnetic thin films do not oxidize.

TABLE I. Important sample properties. ρ_m: mass density; $d_{\rm TEM}$: film thickness determined by TEM; $d_{\rm SE}$: film thickness determined by SE; m: film mass determined by ρ_m and $d_{\rm SE}$; M_s: in-plane saturation magnetization; H_c: coercive field. The H_c offset of H_c is caused by the remanent field in the MPMS superconducting magnet.

Sample	ρ_m (gcm^{-3})	$d_{\rm TEM}$ (nm)	$d_{\rm SE}$ (nm)	m (μg)	M_s (emug^{-1})	H_c [H_c offset] (mT)
Fe	7.87	11.5 (±0.5)	10.5 (±0.09)	1.22 (±0.015)	240 (±2.95)	±3.450 [+1.15]
$Ni_{20}Fe_{80}$	8.00	–	12.0 (±0.10)	3.20 (±0.040)	216 (±2.70)	±2.030 [+1.28]
Co	8.90	–	12.5 (±0.08)	0.96 (±0.009)	140 (±5.82)	±1.780 [+1.22]
$Ni_{80}Fe_{20}$	8.60	14.0 (±0.5)	13.5 (±0.06)	4.30 (±0.029)	76 (±0.51)	±0.100 [+1.26]
Ni	8.91	13.5 (±0.5)	13.5 (±0.05)	2.14 (±0.013)	48 (±0.29)	±0.001 [−0.77]

Using the superconducting quantum interference device (SQUID) magnetometry (Quantum Design, MPMS), we measured the in-plane magnetization of all samples (Fig. 2). The saturation magnetization M_s values (Table I) of Co, Fe, and Ni films are comparable to their bulk values.[26] The M_s of $Ni_{80}Fe_{20}$ and $Ni_{20}Fe_{80}$ films lies in between the M_s of Ni and Fe films, as expected from a linear interpolation of M_s. We observed an offset of coercive field H_c up to ±1.3 mT (Table I). This H_c offset is related to the remanent field in the MPMS superconducting magnet.

Performing the spectroscopic ellipsometry (SE) experiment with VMOGE setup under zero-field condition is sufficient to determine the diagonal terms $\varepsilon_{x,y,z}$ in the MO dielectric tensor $\varepsilon^{\rm MO}$ of the ferromagnetic thin films and in the dielectric tensor of Cr and ZnO. It holds for $\varepsilon_x = \varepsilon_y = \varepsilon_z = (n - ik)^2$. The refractive indices n and the extinction coefficients k (not shown here) agree well with tabulated optical constants of Cr, ferromagnetic materials, and ZnO.[27] The thicknesses $d_{\rm SE}$ of the ferromagnetic thin films determined by SE are also listed in Table I.

III. RESULTS AND DISCUSSION

To study the MO properties of Fe, $Ni_{20}Fe_{80}$, Co, $Ni_{80}Fe_{20}$, and Ni, we performed reflection L-, and T-VMOGE measurements. For the reflection L-VMOGE measurements, an external magnetic field of $H_x = \pm 30$ mT is applied along the x axis, which is sufficiently large to obtain in-plane saturation magnetization of the ferromagnetic films. The Mueller matrix element difference spectra $\Delta M_{ij} = M_{ij}(-H_k) - M_{ij}(H_k)$, $k = x,y,z$ normalized to M_{11} are recorded as a function of wavelength at 50° angle of incidence. Figure 3 shows the experimental and fitted Mueller matrix element difference spectra $\Delta M_{ij}/M_{11}$ of L- and T-VMOGE measurements. An angle of 50° is chosen, as the Mueller matrix elements can be optimized with the angle of incidence near 58°.[1] Nonzero Mueller matrix element difference spectra ΔM_{13}, ΔM_{14}, ΔM_{23}, ΔM_{24}, ΔM_{31}, ΔM_{32} are induced by the external magnetic field H_x. Under the experimental precision of 10^{-4}, ΔM_{13}, ΔM_{24}, and ΔM_{31} are detectable and are given in Fig. 3 (left column). For the 50° reflection T-VMOGE measurements, a magnetic field of $H_y = \pm 30$ mT is applied along the y axis, here a different set of nonzero Mueller matrix element difference spectra (ΔM_{12}, ΔM_{21}, ΔM_{34}) are detected and given in Fig. 3 (right column).

Fitting the experimental Mueller matrix data with the 4×4 transfer matrix method, we obtain the off-diagonal

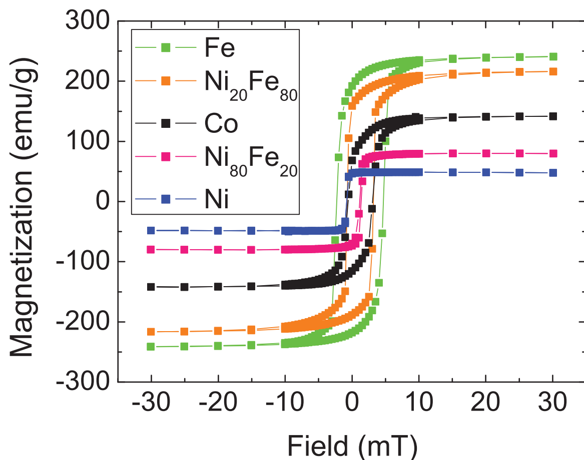

FIG. 2. (Color online) SQUID in-plane magnetization of Fe, $Ni_{20}Fe_{80}$, Co, $Ni_{80}Fe_{20}$, and Ni thin film samples at room temperature. The saturation magnetization M_s and the coercive field H_c are summarized in Table I.

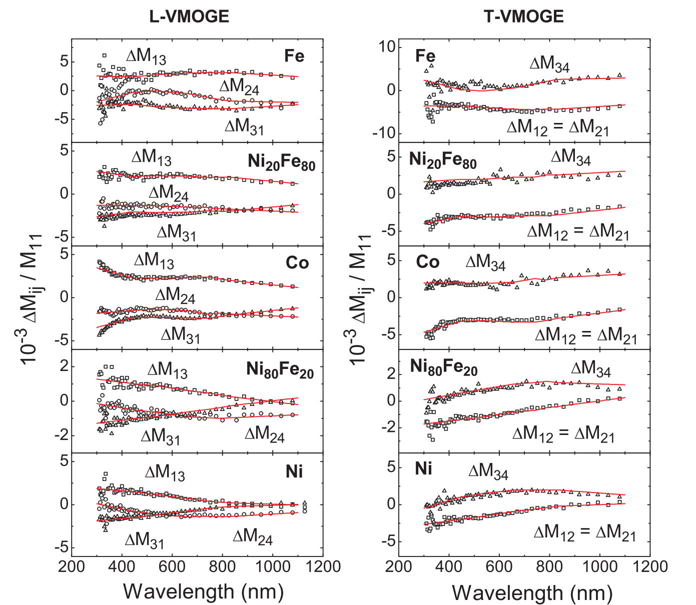

FIG. 3. (Color online) Experimental (symbols) and fitted (line) Mueller matrix element difference spectra $\Delta M_{ij} = M_{ij}(-H_k) - M_{ij}(H_k)$, $i = 1,2,3$, $j = 1,2,3,4$, $k = x,y,z$ normalized to M_{11}, recorded by reflection L- ($H_x = \pm 30$ mT) and T-VMOGE ($H_y = \pm 30$ mT) measurements at 50° angle of incidence on Fe, $Ni_{20}Fe_{80}$, Co, $Ni_{80}Fe_{20}$, and Ni thin film samples.

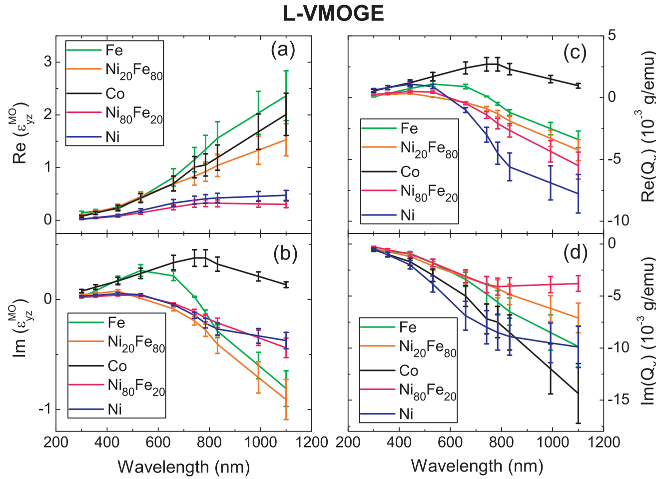

FIG. 4. (Color online) Modeled (a) real and (b) imaginary part of the off-diagonal terms ε_{yz}^{MO} and the extracted (c) real and (d) imaginary part of Q_x of Fe, $Ni_{20}Fe_{80}$, Co, $Ni_{80}Fe_{20}$, and Ni thin films under a magnetic field $H_x = +30$ mT (L-VMOGE) as a function of wavelength. Note that according to Eq. (1), $Re(\varepsilon_{yz}^{MO}) \propto -Im(Q_x)$ [(a) and (d)] and $Im(\varepsilon_{yz}^{MO}) \propto Re(Q_x)$ [(b) and (c)].

terms $\varepsilon_{yz}^{MO} = -iQ_xM_x$ (L-VMOGE) and $\varepsilon_{xz}^{MO} = -iQ_yM_y$ (T-VMOGE) of the ferromagnetic thin films from the best-match model of ε^{MO}. ε_{yz}^{MO} and ε_{xz}^{MO} are identical in this configuration. This indicates that there is no in-plane magneto-optical anisotropy for all the ferromagnetic films. Figures 4(a) and 4(b) show the ε_{yz}^{MO} ($=\varepsilon_{xz}^{MO}$) of all ferromagnetic thin films in the spectral range from 300 to 1100 nm. In order to determine the magnetic-field-independent MO coupling constants Q_x and Q_y, the corresponding saturated in-plane magnetization M_s of the ferromagnetic films is required (Fig. 2). Simply by factoring out the M_s from ε_{yz}^{MO} and ε_{xz}^{MO}, we obtained the identical Q_x and Q_y, respectively [Figs. 4(c) and 4(d)]. According to Eq. (1), $Re(\varepsilon_{ij}^{MO}) \propto -Im(Q_k)$ and $Im(\varepsilon_{ij}^{MO}) \propto Re(Q_k)$ with $k = x,y,z$. Note that Q_z cannot be determined, as the ferromagnetic thin films are not saturated along their hard axis (normal to sample surface). The MO coupling constant **Q** determines how magnetization influences the samples' MO response.[28] Because of isotropic spin-orbit coupling, we expect to obtain isotropic **Q** in the investigated ferromagnetic thin films.

The extracted off-diagonal terms ε_{yz}^{MO} (L-VMOGE) in the MO dielectric tensor of Fe, Co, and Ni are converted in terms of in the optical conductivity tensor σ_{yz}^{MO} using Eq. (2). We show our $\omega\sigma_{yz}^{MO}$ spectra of Fe, Co, and Ni, together with experimental $\omega\sigma_{xy}^{MO}$ spectra reported in Refs. 2,4,17–24 in Figs. 5 and 6. Our experimental results σ_{yz}^{MO} of Fe, Co, and Ni under saturated magnetization conditions in the spectral range of 1–4 eV agree well with the σ_{xy}^{MO} reported in literature. The magneto-optical response is a combined effect of the net spin polarization and electronic band structure of materials, which can be described by the MO dielectric tensor ε^{MO}, or equivalently, with the optical conductivity σ^{MO}. By extracting the magnetic-field-independent MO coupling constant **Q** of a ferromagnetic material, one can predict the MO figure of merit of a MO sensor fabricated from the same ferromagnetic material.

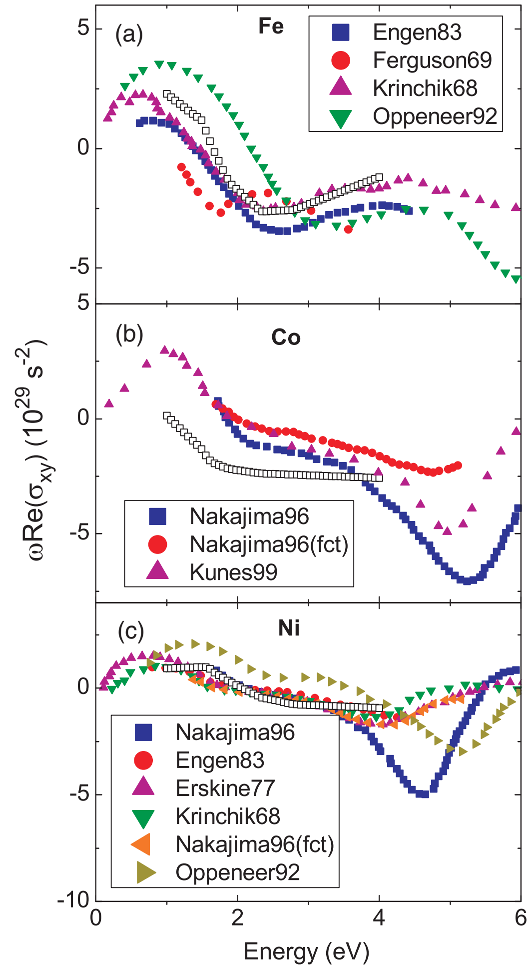

FIG. 5. (Color online) The real part of experimental off-diagonal optical conductivity spectra $\omega\sigma_{xy}^{MO}$ for (a) Fe, (b) Co, and (c) Ni from Refs. 2,4,17–21,23,24. The white squares are the extracted $\omega Re(\sigma_{yz}^{MO})$ of Fe, Co, and Ni, converted from $Im(\varepsilon_{yz}^{MO})$ in Fig. 4(b) by Eq. (2).

Using the determined MO coupling constant **Q**, one can predict the MO response of a multilayer sample structure (e.g., Ni/Fe bilayer, Co/Ni/Co trilayer, and etc.) in terms of the Mueller matrix elements or the complex Kerr angle for a given magnetic field and angle of incidence in the spectral range from 300 to 1100 nm. As an example, Fig. 7 shows the calculated Mueller matrix element difference spectra (ΔM_{13}, ΔM_{24}) and the calculated Kerr angle rotation $\Delta\theta_K$ and ellipticity $\Delta\eta_K$ difference spectra where $\Delta\theta_K = \theta_K(-H_k) - \theta_K(H_k)$ and $\Delta\eta_K = \eta_K(-H_k) - \eta_K(H_k)$, $k = x,y,z$, for Cr(2 nm)/Ni(d_{Ni})/Fe(d_{Fe})/ZnO substrate (solid lines) and Cr(2 nm)/Fe(d_{Fe})/Ni(d_{Ni})/ZnO substrate (dotted lines) multilayer systems with different layer thickness (d_{Fe}, d_{Ni}) as a function of wavelength, in 50° reflection longitudinal configuration under saturated magnetization conditions. The calculated MO data of Cr(2 nm)/Fe, $Ni_{20}Fe_{80}$, $Ni_{80}Fe_{20}$, Ni (10 nm)/ZnO substrate (bold solid lines) are included as a reference. From both the calculated (Fig. 7) and experimental (Fig. 3) data, we observe that in contrast to the saturation magnetization, the MO response of Ni-Fe alloy films cannot be interpolated from the response of pure Ni and Fe films. As for the multilayer systems, a linear interpolation with a

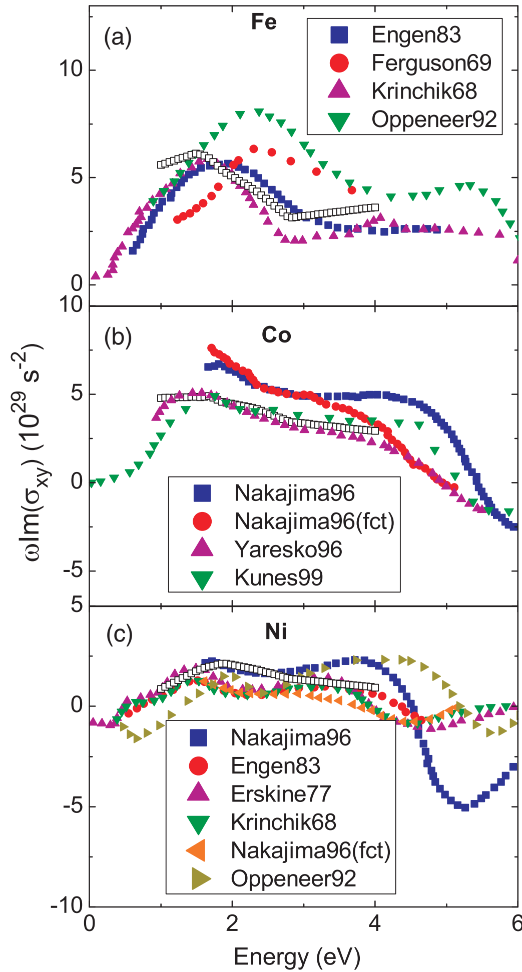

FIG. 6. (Color online) The imaginary part of experimental off-diagonal optical conductivity spectra $\omega\sigma_{xy}^{\mathrm{MO}}$ for (a) Fe, (b) Co, and (c) Ni from Refs. 2,4,17–24. The white squares are the extracted $\omega Im(\sigma_{yz}^{\mathrm{MO}})$ of Fe, Co, and Ni, converted from $Re(\varepsilon_{yz}^{\mathrm{MO}})$ in Fig. 4(a) by Eq. (2).

controlled MO response may be realized by choosing the thickness of each layer (d_{Fe}, d_{Ni}) such that the total thickness ($d_{\mathrm{Fe}} + d_{\mathrm{Ni}}$) is similar to the single Ni or Fe film thickness. Furthermore, for a given angle of incidence, one can select an optimal wavelength such that the MO response of a specific ferromagnetic material is maximal. Once the experimental conditions for this MO response have been benchmarked, the nature of coherence and damping in ferromagnetic systems can be investigated by magnetodynamic measurements[29] with maximum MO response.

IV. CONCLUSION

Magneto-optical properties of Fe, $Ni_{20}Fe_{80}$, Co, $Ni_{80}Fe_{20}$, and Ni thin films have been studied by vector-magneto-optical generalized ellipsometry measurements under saturated magnetization conditions in the sample surface plane. Mueller matrix ellipsometry has been performed and the off-diagonal elements of the MO dielectric tensor $\varepsilon^{\mathrm{MO}}$, or equivalently of the optical conductivity σ^{MO} have been determined by model analysis. The combined effect of net spin polarization and electronic band structure of materials can be described by $\varepsilon^{\mathrm{MO}}$(or σ^{MO}). In addition with the SQUID magnetization data, the wavelength-dependent, magnetic-field-independent, and complex MO coupling constants Q_x and Q_y have been evaluated. For a given magnetization $\mathbf{M}$, the MO response of a ferromagnetic multilayer sample can be predicted, and a controlled MO response can be obtained by choosing thickness and material of each ferromagnetic layer.

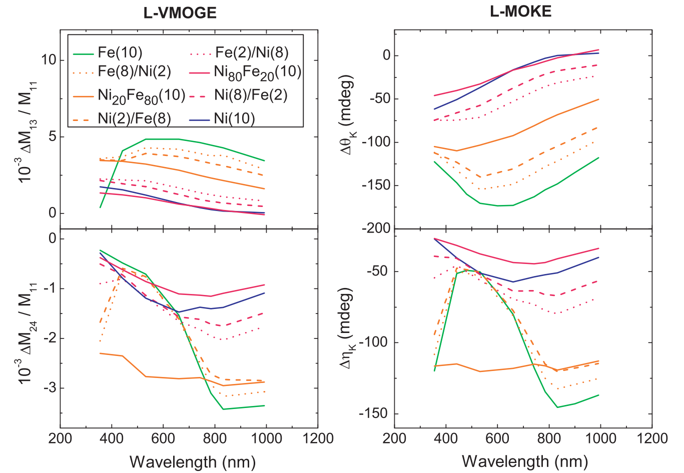

FIG. 7. (Color online) The calculated Mueller matrix elements ΔM_{13} and ΔM_{24} (left column: compare with Fig. 3 left column), as well as the Kerr rotation $\Delta\theta_K$ and ellipticity $\Delta\eta_K$ (right column) of Cr(2 nm)/Ni(d_{Ni})/Fe(d_{Fe})/ZnO substrate (solid lines) and of Cr(2 nm)/Fe(d_{Fe})/Ni(d_{Ni})/ZnO substrate (dotted lines) multilayer samples under saturated magnetization conditions, as a function of wavelength, in 50° reflection longitudinal configuration. The calculated MO data of the alloy Cr(2)/Fe, $Ni_{20}Fe_{80}$, $Ni_{80}Fe_{20}$, Ni (10)/ZnO substrate multilayer samples (bold solid lines) are taken as a reference. The single layer thickness is indicated in brackets in units of nm.

In our work, we discussed ferromagnetic thin film samples, which have the relation of magnetic field and magnetization $M_k(H_k)$, $k = x,y,z$. Indeed, it is very difficult to model more complicated anisotropic films with relation between magnetization and magnetic field $M_k(H_l), k,l = x,y,z$ and to factor out the wavelength-dependent, magnetic-field-independent MO coupling constants $\mathbf{Q}$ from the nonsymmetric terms $\varepsilon_{ij}^{\mathrm{MO}}$. So far, the vector Preisach model has been used to extract the magnetization $M_k(H_l)$ of anisotropic samples from a series of magnetization measurements. By factoring out the experimentally determined $M_k(H_l)$ from the nonsymmetric terms $\varepsilon_{ij}^{\mathrm{MO}}$, the anisotropic MO coupling constant $\mathbf{Q}$ can be obtained and conclusions regarding the net spin polarization and electronic band structure of complicated anisotropic films can be drawn.

ACKNOWLEDGMENTS

The authors acknowledge financial support from the Bundesministerium für Bildung und Forschung (Grant No. FKZ 13N10144) and the Deutsche Forschungsgemeinschaft (Grant No. SCHM1663/1-2). We also thank T. Scheumann and I. Skorupa from HZDR for the sample preparation, D. Bürger from HZDR for the help with SQUID measurements, and M. Gensch from HZDR for fruitful discussions.

*kelvinmok@hzdr.de

[1]K. Mok, N. Du, and H. Schmidt, Rev. Sci. Instrum. **82**, 033112 (2011).
[2]P. M. Oppeneer, T. Maurer, J. Sticht, and J. Kübler, Phys. Rev. B **45**, 10924 (1992).
[3]T. Gasche, M. S. S. Brooks, and B. Johansson, Phys. Rev. B **53**, 296 (1996).
[4]A. Delin, O. Eriksson, B. Johansson, S. Auluck, and J. M. Wills, Phys. Rev. B **60**, 14105 (1999).
[5]H.-C. Mertins, S. Valencia, D. Abramsohn, A. Gaupp, W. Gudat, and P. M. Oppeneer, Phys. Rev. B **69**, 064407 (2004).
[6]A. Berger and M. R. Pufall, Appl. Phys. Lett. **71**, 965 (1997).
[7]G. Neuber, R. Rauer, J. Kunze, T. Korn, C. Pels, G. Meier, U. Merkt, J. Bäckström, and M. Rübhausen, Appl. Phys. Lett. **83**, 4509 (2003).
[8]R. Rauer, G. Neuber, J. Kunze, J. Bäckström, and M. Rübhausen, Rev. Sci. Instrum. **76**, 023910 (2005).
[9]T. Hofmann, U. Schade, C. M. Herzinger, P. Esquinazi, and M. Schubert, Rev. Sci. Instrum. **77**, 063902 (2006).
[10]G. E. Jellison and F. A. Modine, Appl. Opt. **36**, 8190 (1997).
[11]H. Fujiwara, *Spectroscopic Ellipsometry, Principle and Applications* (Wiley, Japan, 2007).
[12]M. Schubert, *Infrared Ellipsometry on Semiconductor Layer Structures: Phonons, Plasmons and Polaritons* (Springer, Berlin, 2005).
[13]M. Schubert, Phys. Rev. B **53**, 4265 (1996).
[14] Š. Višňovský, K. Postava, and T. Yamaguchi, Czech. J. Phys. **51**, 917 (2001).
[15]M. Schubert, Thin Solid Films **313–314**, 323 (1998).
[16]X. Gao, J. A. Woollam, R. D. Kirby, D. J. Sellmyer, C. T. Tanaka, J. Nowak, and J. S. Moodera, Phys. Rev. B **59**, 9965 (1999).
[17]P. G. V. Engen, Ph.D. thesis, Technical University Delft, 1983.
[18]P. E. Ferguson and R. J. Romagnoli, J. Appl. Phys. **40**, 1236 (1969).
[19]G. S. Krinchik and V. A. Artemjev, J. Appl. Phys. **39**, 1276 (1968).
[20]K. Nakajima, H. Sawada, T. Katayama, and T. Miyazaki, Phys. Rev. B **54**, 15950 (1996).
[21]J. Kuneš and P. Novăk, J. Phys. Condens. Matter **11**, 6301 (1999).
[22]S. Uba, L. Uba, A. N. Yaresko, A. Y. Perlov, V. N. Antonov, and R. Gontarz, Phys. Rev. B **53**, 6526 (1996).
[23]J. L. Erskine, Physica B & C **89**, 83 (1977).
[24]D. Martin, S. Doniach, and K. Neal, Phys. Lett. **9**, 224 (1964).
[25]H. Regensburger, R. Vollmer, and J. Kirschner, Phys. Rev. B **61**, 14716 (2000).
[26]E. P. Wohlfarth, *Ferromagnetic Materials* (North-Holland, Amsterdam, 1980).
[27]E. D. Palik, *Handbook of Optical Constants of Solids* (Academic Press, San Diego, 1998).
[28]T. Kampfrath, R. G. Ulbrich, F. Leuenberger, M. Münzenberg, B. Sass, and W. Felsch, Phys. Rev. B **65**, 104429 (2002).
[29]E. Beaurepaire, J.-C. Merle, A. Daunois, and J.-Y. Bigot, Phys. Rev. Lett. **76**, 4250 (1996).